Last galley proof enclosed

Journal Article

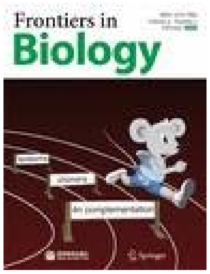

On governance in the long-term vegetation process: How to discover the rules?

Journal	Frontiers of Biology in China
Publisher	Higher Education Press, co-published with Springer-Verlag GmbH
ISSN	1673-3509 (Print) 1673-3622 (Online)
Issue	Volume 4, Number 4 / December, 2009
Category	Research Article
DOI	10.1007/s11515-009-0057-y
Pages	557-568
Subject Collection	Biomedical and Life Sciences
SpringerLink Date	Wednesday, September 16, 2009

PDF (397.5 KB) Free Preview

László Orlóci[1] and **Kate S. He**[2]

(1) Departamento de Ecologia, Universidade Federal do Rio Grande do Sul, Porto Alegre, RS, 91540-000, Brazil

(2) Department of Biological Sciences, Murray State University, Murray, KY 42071, USA

Received: 30 April 2009 **Accepted:** 10 June 2009 **Published online:** 10 September 2009

Abstract Ecological practice is telling us that to identify Nature's rules, we should look for regularities in the resulting effects. Hidden rules are involved and the effects are manifested by compositional, functional, and structural transitions. This paper's focus is on two conjectures regarding the governance of specific transition components, the first supposedly under global co-ordination, and the second under superimposed site specific instability oscillations. The reality of any apparent regularity in these is the sole condition for the regularity's acceptance as a rule. Reality is testable but in retrospect only, based on time series analyses. Since long pollen spectra supply the evidence, the time period involved is measured in thousands of years. For maximal usefulness, a spectrum should have a long period length, dated horizons intensely sampled at short time steps, and precisely identified taxa. Period length and time step width matter because both may have a masking effect on the regularities. There is, of course, a natural limit for period length, which is set by the age of the pollen bearing sediments. We completed the analysis of 23 spectra using techniques deemed suitable for testing the conjectures. The spectra originated from sites in the Americas where we found suitable spectra in sufficient numbers and in geographic contiguity from the Arctic region to the Antarctic. The presented results have clear indications that the two conjectures identify real rules. The main body of the paper narrates the analyses and provides explanations. Informative materials, too voluminous for inclusion in the paper, are made available on the Internet at URL: www.vegetationdynamics.com linking to "Appendices Ta".

Keywords governance - long-term process - vegetation - rules

László Orlóci
Email: laszlo.orloci@gmail.com

Fulltext Preview (Small, Large)

Front. Biol. China
DOI 10.1007/s11515-009-0057-y

RESEARCH ARTICLE

On governance in the long-term vegetation process: How to discover the rules?

László ORLÓCI (✉)[1], Kate S. HE[2]

1 Departamento de Ecologia, Universidade Federal do Rio Grande do Sul, Porto Alegre, RS, 91540-000, Brazil
2 Department of Biological Sciences, Murray State University, Murray, KY 42071, USA

Abstract Ecological practice is telling us that to identify Nature's rules, we should look for regularities in the resulting effects. Hidden rules are involved and the effects are manifested by compositional, functional, and structural transitions. This paper's focus is on two conjectures regarding the governance of specific transition components, the first supposedly under global co-ordination, and the second under superimposed site specific instability oscillations. The reality of any apparent regularity in these is the sole condition for the regularity's acceptance as a rule. Reality is testable but in retrospect only, based on time series analyses. Since long pollen spectra supply the evidence, the time period involved is measured in thousands of years. For maximal usefulness, a spectrum should have a long period length, dated horizons intensely sampled at short time steps, and precisely identified taxa. Period length and time step width matter because both may have a masking effect on the regularities. There is, of course, a natural limit for period length, which is set by the age of the pollen bearing sediments. We completed the analysis of 23 spectra using techniques deemed suitable for testing the conjectures. The spectra originated from sites in the Americas where we found suitable spectra in sufficient numbers and in geographic contiguity from the Arctic region to the Antarctic. The presented results have clear indications that the two conjectures identify real rules. The main body of the paper narrates the analyses and provides explanations. Informative materials, too voluminous for inclusion in the paper, are made available on the Internet at URL: www.vegetationdynamics.com linking to "Appendices Ta".

Received April 30, 2009; accepted June 10, 2009

E-mail: laszlo.orloci@gmail.com

Keywords governance, long-term process, vegetation, rules

1 Introduction

The conjecture of regional parallelism as a series of co-ordinated compositional transitions can be traced back to the early decades of the 20^{th} century. The idea is comprehensively articulated by von Post (1946) in his account of studies regarding the compositional structure of long pollen spectra. In von Post's comparative analytical approach, the task of studying long-term structural change in parallel samples was hindered by the lack of comparable taxonomic composition. Von Post's solution to this problem involves a re-definition of compositional transitions in terms of new, generalized taxa of two types, which he named *mediocritic* and *terminocritic*. Based on these taxa, von Post could uncover a fundamental global regularity for which his term is *revertence*. Our term for the same is "Globally co-ordinated periodicity" . Changes are involved in the course of which specific structures and relationships rise, fall, and resurface in cycles.

Von Post's (1946) ideas have considerable relevance in global change studies today. They stimulated the development of *trajectory analysis* (*TA*). This is an entire family of novel, powerful statistical techniques for time series analysis (He and Orlóci, 1999; Orlóci et al., 2002, 2006; Orlóci, 2009) designed for the study of long term vegetation dynamics. *TA* creates a phase space[1)] mapping for each spectrum and uses the mappings as surrogate series of the real process. *TA*'s analytical tools were designed to probe the mappings for ecologically meaningful regularities and to turn the trajectory's morphological characteristics into the vegetation indicators of critical environmental change. *TA's modus operandi* is in

1) A time-by-palynomorphs reference space in which a series (trajectory) of compositional transitions defines the time axes.

Look for the definitive version as a First on Line Publication in Frontiers of Biology in Chine, Higher Education Press and Springer-Verlag ~~2009~~

On governance in the long-term vegetation process: How to discover the rules?

László ORLÓCI (✉)[1*] , Kate S. HE[2]

1 Departamento de Ecologia, Universidade Federal do Rio Grande do Sul, Porto Alegre, RS, 91540-000, Brazil

2 Department of Biological Sciences, Murray State University, Murray, Kentucky 42071, USA

Abstract Ecological practice is telling us that to identify Nature's rules, we should look for regularities in the resulting effects. Hidden rules are involved and the effects are manifested by compositional, functional, and structural transitions. The paper's focus is on two conjectures regarding the governance of specific transition components, the first supposedly under global co-ordination, and the second under superimposed site specific instability oscillations. The reality of any apparent regularity in these is the sole condition for the regularity's acceptance as a rule. Reality is testable but in the retrospect only, based on time series analyses. Since long pollen spectra supply the evidence, the time period involved is measured in thousands of years. For maximal usefulness, a spectrum should have long period length, dated horizons intensely sampled at short time steps, and precisely identified taxa., Period length and time step width

---

Received April 30, 2009; accepted June 10, 2009
E-mail: laszlo.orloci@gmail.com

URL: http://vegetationdynamics.com

matter because both may have a masking effect on the regularities. There is, of course, a natural limit for period length, which is set by the age of the pollen bearing sediments. We completed the analysis of 23 spectra using techniques deemed suitable for testing the conjectures. The spectra originate from sites in the Americas where we found suitable spectra in sufficient numbers and in geographic contiguity from the Arctic region to the Antarctic. The presented results have clear indications that the two conjectures identify real rules. The main body of the paper narrates the analyses and provides explanations. Informative materials, too voluminous for inclusion in the paper, are made available on the Internet at URL: www.vegetationdynamics.com linking to "Appendices Ta".

Keywords governance, long-term process, vegetation, rules

1 Introduction

The conjecture of regional parallelism as a series of co-ordinated compositional transitions can be traced back to the early decades of the 20th century. The idea is comprehensively articulated by von Post (1946) in his account of studies regarding the compositional structure of long pollen spectra. In von Post's comparative analytical approach, the task of studying long-term structural change in parallel samples was hindered by the lack of comparable taxonomic composition. Von Post's solution to this problem involves a re-definition of compositional transitions in terms of new, generalized taxa of two types, which he named *mediocritic* and *terminocritic*. Based on these taxa, von Post could uncover a fundamental global regularity for which his term is *revertence.* Our term for the same is "Globally co-ordinated periodicity" . Changes are involved in the course of which specific structures and relationships rise, fall, and resurface in cycles.

Von Post's (1946) ideas have considerable relevance in global change studies today. They stimulated the development of *trajectory analysis* (*TA*). This is an entire family of novel, powerful statistical techniques for time series analysis (He and Orlóci, 1999; Orlóci et al., 2002, 2006; Orlóci 2009) designed for the study of long term vegetation dynamics. *TA* creates a phase space[1] mapping for each spectrum and uses the mappings as surrogate series of the real process. *TA's* analytical tools were designed to probe the mappings for ecologically meaningful regularities and to turn the trajectory's morphological characteristics into the vegetation indicators of critical environmental change. *TA's modus operandi* is in complete conformity with current needs in global change science: it is multi-scale, multivariate, and probabilistic.

We extend the scope of trajectory analysis in this paper into the area of probabilistic reality tests. Since in the von Post conjecture trajectory directionality is implied, the conjecture is testable for reality on that basis. Our conjecture concerning the local rule of governance over compositional instability oscillations implies compositional transition velocity oscillations and can be tested on that basis.

2 Data sources, types, and reliability

We use palynomorphs as proxies for taxa and palynomorph quantities to estimate the composition of the paleo plant community. The horizon dates give us the time scale. The sites and data sets are described in Table 1. Figure 1 has the site map.

Table 1 Description of the pollen spectra

#	location and abbreviation	contact person	geographic cordinates	ele- vation above	number of palyno-	period length yr	PCA* %	eco- region	precipitation midrange (PREC) and	PREC/PET

[1] A time-by-palynomorphs reference space in which a series (trajectory) of compositional transitions defines the time axes.

				sea level m	morphs and Time steps				Potential evapo-transpiration (PET) midrange mm	
1	Hanging Lake, Yukon (HA)	Cwynar 1982	68.23.00N 138.23.00W	500	89 x 133 3x412	0-41138	88.9	T	125 200	0.63
2	Kaiyak Lake, Alaska (KAI)	Anderson (1985)	68.09.00N 161.25.00W	190	66 x 53 3x394	0-39392	97.7	T	125 200	0.63
3	Joe Lake, Alaska (JOE)	Anderson (1988)	66.46.00N 157.13.00W	183	90 x 87 3x439	0-43804	93.5	T	375 200	1.88
4	John Klondike Bog, Yukon (JKL)	Matthews (1980)	60.21.24N 123.38.48W	460	47 x 43 3x97	0-9620	87.2	B	375 600	0.63
5	Beaverhouse Lake, Manitoba (FF)	Ritchie (1976)	54.44.32N 101.40.54W	305	67 x 53 3 x 91	0-9000	95.4	B	375 600	0.63
6	E Lake, Manitoba (EL)	Ritchie (1964)	59.41.29N 99.39.30W	735	48 x 57 3 x 115	0-11422	97.5	B	375 1000	0.38
7	Lac Yelle, Ontario (YEL)	McAndrews (1981)	48.30.14N 79.38.16W	356	86 x 32 3 x 93	0-9200	97.7	B	125 1000	0.13
8	Rice Lake, North, Dakota (RIC)	Grimm, E.C .*	48.00.29N 101.31.49W	620	111 x 88 3 x 97	0-9693	98.3	G	125 1000	0.13
9	Cheyenne Bottoms, Kansas (CHE)	Fredlung (1995)	38.28.00N 98.4000W	547	76 x 100 3 x 98	0-22648	96.3	G	750 1000	0.75
10	Hay Lake, Arizona (HAY)	Jacob (1985)	34.00.00N 109.25.30W	2780	44 x 46 3 x 446	106-44692	84.9	D	125 1000	0.13
11	Boriack Bog, Texas (BOR)	Bryant (1977)	30.21.36N 97.0734W	143	40 x 55 3 x 163	0-16201	92.0	D	125 1400	0.09
12	Lake Tulan, Florida (TUL)	Grimm (1993)	27.35.00N 81.30.00W	34	163x190 3x520	0-51670	98.8	TS	1250 1400	0.89
13	Lake Patzcuaro, Mexico (PAT)	Watts (1982)	19.35.00N 101.35.00W	2044	53x64 3x441	0-44100	92.5	D	750 1000	0.75
14	Paramo de Miranda, Venezuela (PAR)	Salgado-Labouriau (1988)	8.55.00N 70.50.00W	3209	52x37 3x157	37-15601	96.7	S	1250 1000	1.25
15	Lagoa das Patas, Amazonas (LDP)	Colinvaux et al. (1996)	00.16.00N 66.41.00W	300	150x49 3x446	0-44569	77.0	TE	1750 1800	0.97
16	Morro de Itapeva, Sao Paulo (ITA)	Behling, H.*	22.47.00S 45.32.00W	1850	152x43 3351	0-35005	95.3	TS	1250 1000	1.25
17	Cambará, Rio Grande do Sul (CAM)	Behling et al. (2004)	23.03.09S 50.06.04W	1046	164x190 3x379	0-37916	93.4	TS	1250 1000	1.25
18	Serra Campos Gerais,	Behling (1997)	24.40.00S 50.13.00W	1200	147x27 3x125	0-12480	95.4	TS	1250 1000	1.25

	Paraná (GER)									
19	Serra da Boa Vista, Santa Catarina (BOA)	Behling (1995)	27.42.00S 49.09.00W	1160	82x38 3x142	0-14191	99.6	TS	1250 1000	1.25
20	Vaca Lauquen, Néuquen (VAC)	Markgraf (1987)	36.50.00S 71.05.00W	1450	66x36 3x113	0-11258	89.8	TD	750 1000	0.75
21	Mallin Book, Rio Negro (MAL)	Markgraf (1983)	41.20.00S 71.35.00W	800	6x63 3x142	0-14195	99.1	D	375 1000	0.38
22	La Mision, Tierra del Fuego (MIS)	Markgraf (1983)	53.30.00S 67.50.00W	5	45x64 3x118	0-11730	98.9	D	375 1000	0.38
23	Harberton, Tierra del Fuego (HAR)	Markgraf (1989)	54.53.ooS 67.10.00W	20	33x81 3x135	0-13464	97.5	D	375 1000	0.38

The data sources are identified in the main text. The palynomorphs are taxa identified as pollen, spore, and other plant tissue types. *PCA%* is the efficiency of three principal components (generalised palynomorhps) in accounting for total variation in the set of all palynomorphs. Other symbols: T –Tundra and Taiga; B – Boreal Evergreen and Boreal Seasonal; G –Grassland; S – Shrub; D – Semi desert; TE – Tropical Evergreen; TS – Tropical Seasonal; TD– Temperate Seasonal. See Figure 1 for map of geographic locations.
*See comments regarding the marked references in the text below.

The first question of the reader may very well be, why do we limit the data set to the spectra from the Americas. Our reason is the availability of suitable spectra in sufficient numbers and relatively high geographic contiguity from the Arctic to Antarctic. Our main source for pollen spectra is the Global Pollen Database (2009 URL: www.ncdc.noaa.gov/paleo/ftp-pollen.html). One exception is the Cambará spectrum which H. Behling kindly made available to L.O. for use by earlier papers (Orlóci et al. 2002, 2006). The Global Pollen Database does not indicate any published reference for the Grimm, E.C. spectrum.

A typical pollen spectrum is displayed in the Webb-based Appendix K link of URL www.vegetationdynamics.com. It is a stepwise time series of compositional transitions, frugally reduced to the top 15 leading palinomorphs. In the full data set, compositional transitions are recorded for 49 palynomorphs in 150 time steps from recent time back to 44.5 k yr BP. The period length differs substantially (see Table 1). Ten of the 23 spectra span the major cooling and warming cycles of the Late Quaternary. Seven spectra reach back in time from present to the

Globe's emergence from the last Ice Age. The period length of the remaining spectra coincides roughly with the present Interglacial Epoch.

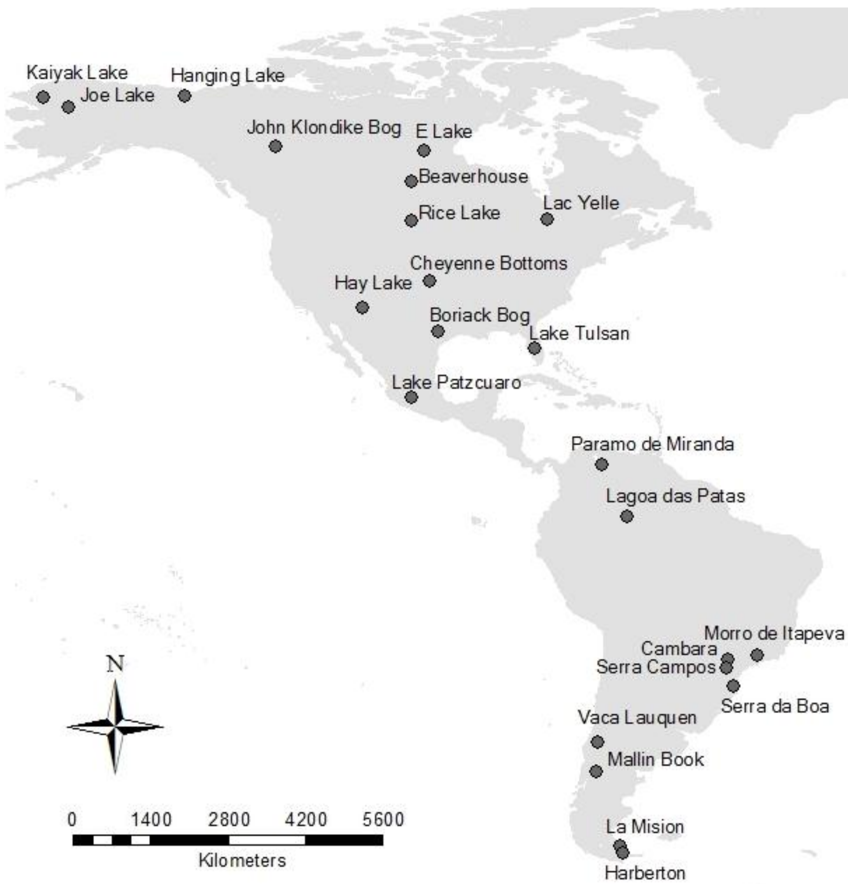

Fig. 1 Site map of the 23 pollen spectra (see details in Table 1)

The environmental data sources include: current mean annual precipitation (2007 URL: www.worldclimate.com and the 2009 URL: www-cger.nies.go.jp/grid-e/gridtxt/grid13.html); current mean annual potential evapotranspiration (UNEP/GRID and UEA/CRU data bases, 2008 URL: www-cger.nies.go.jp/grid-e/gridtxt/pet.html alternatively www-cger.nies.go.jp/grid-e/gridtxt/tateishi.html); current global vegetation cover map (Lapola et al., 2008);; deuterium-based temperature readings (Vostok series, Petit et al., 1999; 2009 URL: ftp.ncdc.noaa.gov/pub/data/paleo/icecore/antarctica/vostok/deutnat.txt).

How reliable are the palynological records? They are not perfect. But, no other information source exists in such impressive numbers and with such level of geographic contiguity to serve our purpose. In fact, without the pollen, spore, and other organic tissue records extracted from sediments, science would know very little about the Late Quaternary history of the Earth's vegetation cover. Palynological data are known for errors from many sources (He and Orlóci, 1999; Orlóci et al., 2002, 2006; Orlóci, 2008). These are linked to (1) the type of dispersal of pollen, spore and other organic tissue without geographic boundaries under much random influence, (2) problematic identification of materials in different states of decay, (3) estimation of the quantities of the different palynomorph types, and (4) the near impossibility of distinguishing the organic matter in the sediments by origin, whether strictly local or transported.

An interesting point can be made about palynomorph taxa in relation to other types of taxa which we use in ecology. The species-based taxa are noted at least in intent for homogeneous inheritance. But there can be taxa of other kinds recognised as, for example, functional types. We provide examples of non-species based taxa in earlier papers (Orlóci, 1991; Pillar and Orlóci, 1993a,b). The fact that palynomorph taxa are neither species-based nor have homogeneous functionality, need not be a reason for undermining their ecological utility. In support of this claim we mention our success to find links between compositional structures in the palynomorph collections of spectra and the long series of oscillations in the global atmospheric temperature, regional humidity, aridity, and anthropogenic effects.

The precision of the palynological records are judged low by the measurement standards of physical science. Most survey type ecological data suffer the same judgment. It must, however, be born in mind that the only data available to us for the purposes we defined is the type that paleobotanists and paleoecologists collect and publish. Since we obtained the spectra from published sources, screened in peer review, we should have no compelling reason to regard the data we use anything, but completely acceptable based on the prevailing scientific standards of the field.

3 Scaling parallelism and instability

The non-identical composition of the palynomorph collections in the different spectra and the palynomorphs' complex non-linear correlation structure create a hard-to-manage reference frame for statistical analysis. The same fact excludes the logical application of many powerful comparative techniques, such as for example, Morrison's (1976) mathematically elegant probabilistic profile analysis.

Starting from the non-conventional reference frame, trajectory analysis takes on a number of unique statistical tasks. It begins with probing the time series of compositional transitions for global parallelism. Our parallelism scalar is a fraction, $TSC = \frac{FMDT}{TNDT}$ to which we refer as the *topological similarity coefficient*[2]. Counts of shared forward (++) or backward (- -) compositional shifts, or no shifts at all (00) along the time axis supply the elementary data. The palynomorph axes or their transforms are taken in pairs, *a* from spectrum *A* and *b* from spectrum *B*. The following is an abbreviated description of the algorithm:

[2] 'Topological' is the term linking similarity with the general notion of topography. 'Topology' is the study of the topography of objects as in land surveying, landscape ecology, trajectory morphology, etc. 'Topology' is definitely not intended here as a term to imply the mathematician's geometry on a 'rubber sheet' as S. Smale has used it, making vivid the nature of the concept.

(1) tGeneralized palynomorphs (*GPMs*) are defined. These are the principal components of the palynomorphs-by-palynomorphs centered product matrix (Orlóci, 1978). We apply equal time step transformation to the spectra prior to the Principal Components Analysis (*PCA*). This way we establish comparability of the time points between the spectra. The criterion for pairing *GPMs*, *a* of *A* with *b* of *B,* is a product moment correlation coefficient which the pairs maximize. The number of *GPMs* in the analysis is uniformly 3. We found that the three principal components corresponding to the three largest generalized variances (characteristic roots, Eigenvalues) of the product matrix is sufficiently accurate. Table 1 lists the total % variation accounted for by the principal component triplets.

(2) Symbols *FMDT* and *TNDT* represent the frequency of matching directional transitions (++, --, 00) and the total number of directional transitions actually examined. We explain the notion of directionality and directionality counts in symbolic terms in (3) below, according to data unit positions in the time series:

Time point	t	$t+1$	...
Data points of palynomorph *a* of spectrum *A*	a_t	a_{t+1}	...
Data points of palynomorph *b* in spectrum *B*	b_t	b_{t+1}	...

(3) In the next step, we count the matches according to specific directionality rules. The algebraic conventions used below follow the technical code of John G. Kemény and Thomas E. Kurtz used in their True Basic programming language (http://www.truebasic.com):

```
DO
   IF abs(at-at+1) < = TR and abs(bt-bt+1) < = TR then
      LET FMDT = FMDT+1
      LET TNDT = TNDT+1
      EXIT DO
   ELSE
      IF at < at+1 and bt < bt+1 or at > at+1 and bt > bt+1 then
         LET FMDT = FMDT+1
         LET TNDT = TNDT+1
         EXIT DO
```

```
        END IF
    END IF
    LET FMDT = FMDT+1
    EXIT DO
LOOP
```

(4) The notion of multiscaling is linked with the increasing radius *TR* of a tolerance sphere around each data point, such that *TR = q, q+d, q+2d, ..., maxTR* in the palynomorphs' measurement units.

(5) *FMDT* and *TNDT* accumulate the counts as we go through all *GPM* pairs for computation of a new *TSC* value at each *TR*. Then we re-compute all *TSC* many times over in the same manner each time as before, but each time starting with a new randomization of the data points' time series positions. The confidence limits (*UL*, *LL*) and expectations (*E*) are the outcome of the repeated randomization.

(6) The construction of graphs such as in Fig. 2 concludes this phase of the analysis.

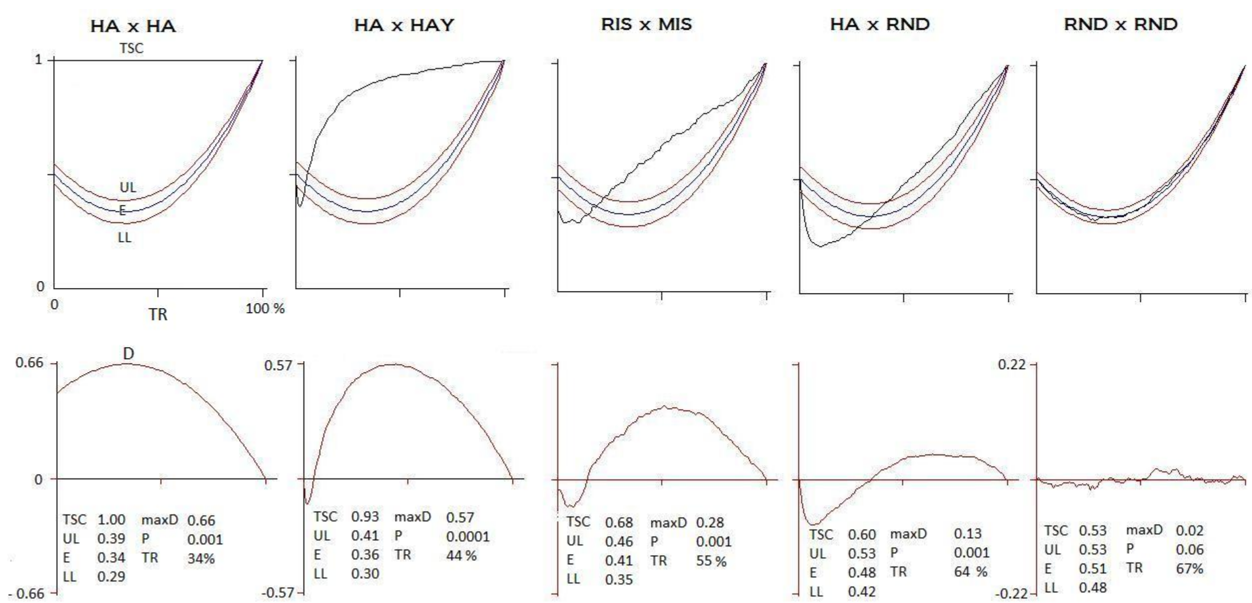

Fig. 2 Graphs of the topological similarity coefficient *(TSC)* for selected pairs of spectra as identified. Code names of spectra and other site details are given in Table 1. Horizontal axis (*TR*): % scale for tolerance radius. Curves: *UL*, *LL* – upper and lower limits of the 1-α = 0.95 probability confidence belt around random expectation (*E*); *D* = *TSC* -

E. Columns: HA x HA – Hanging Lake spectrum compared to itself; HA x HAY – Hanging Lake spectrum compared to the Hay Lake spectrum; RIS x MIS – Rice Lake spectrum compared to the La Mision spectrum; HA x RND – Hanging Lake spectrum compared to a case of random compositional walk; RND x RND – random compositional walk compared to random compositional walk. Other symbols: *maxD* – the maximum value of *D* (graphs in 2nd row); *P* – the probability that any *maxD* value occurring under the regularity condition of random compositional transitions will be equal to or exceed the natural *maxD* value actually observed. Note, the straight *TSC* line at 1.0 in the first graph. This is typical in the comparison of identical spectra. The *maxD* of identical spectra is 0.66. Important note: all graphs are based on spectra with time steps adjusted to 100 yr. Expectations, confidence limits and probabilities are determined in Monte Carlo simulations involving 1000 iterations and 1% stepwise increments in *TR*. At this number of iterations the values should be approaching stability rather closely.

(7) Finally, we find the possible upper limit of *D* = *TSC-E* in self comparisons. This upper limit turned out to be *0.66* uniformly in all cases. The individual *D* values as fractions of *0.66* are direct expressions of the extent to which the maximum possible value of *TSC-E* is approached in any of the spectra.

The determination of expectations (*E*), probabilities (α), and confidence limits (*UL*, *LL*,) requires further computational steps. The methodology is known to statisticians as the Monte Carlo simulation. Regarding the general idea, sufficient details are presented by Hammersley and Handscomb (1964) not to have to deal with the theory to any length in this paper. In the ecological practice the method's implementations involve different types of randomization. We applied random permutation to the data points' time sequence. The basic number of permuted sets is one thousand. We consider this number quite sufficient to obtain reasonably stable results.

The *TSC* graph segments above the *UL* line (see Fig. 2) indicate significant parallelism. But the conclusion that process parallelism is real does not exclude possibly significant site specific differences between the spectrs in other important characters characteristics. Site-sensitive process instability is one of this particular character domain. A well-tested scalar for process instability is *compositional transition velocity* which we present in the angular form by

$V = \frac{\cos^{-1}\left(1 - \frac{d^2}{2}\right)}{|t_a - t_b|}$. V is measured in radians/time and d^2 is the squared compositional chord distance (Orlóci, 1978) of two consecutive compositional states a,b at time points t_a and t_b . Implicit in the chord distance is normalization (the setting of state vector length equal to unity).The co-ordinate system's origin is kept at the original zero point. Noting that the values of $\cos^{-1}\left(1 - \frac{d^2}{2}\right)$ range from *0* to *π/2,* the V values are directly comparable within and between spectra. Another important point to mention is that large V values indicate high compositional instability and small V values indicate high compositional stability.

Another instability measure is the *compositional transition acceleration/deceleration,* $A = \frac{V_{t+\Delta t} - V_t}{\Delta t}$. When A is positive, acceleration occurs within the Δt time interval. A negative A indicates deceleration. Put it in another way, $A > 0$ signals increasing compositional transition instability. By the same token, $A < 0$ indicates increasing stability. Both A and V are ecologically meaningful measures (Orlóci et al., 2002, 2006; Orlóci, 2009). V and A values can locate hotspots of change in time and space. Figure 3 contains V and A oscillograms for the type spectra.

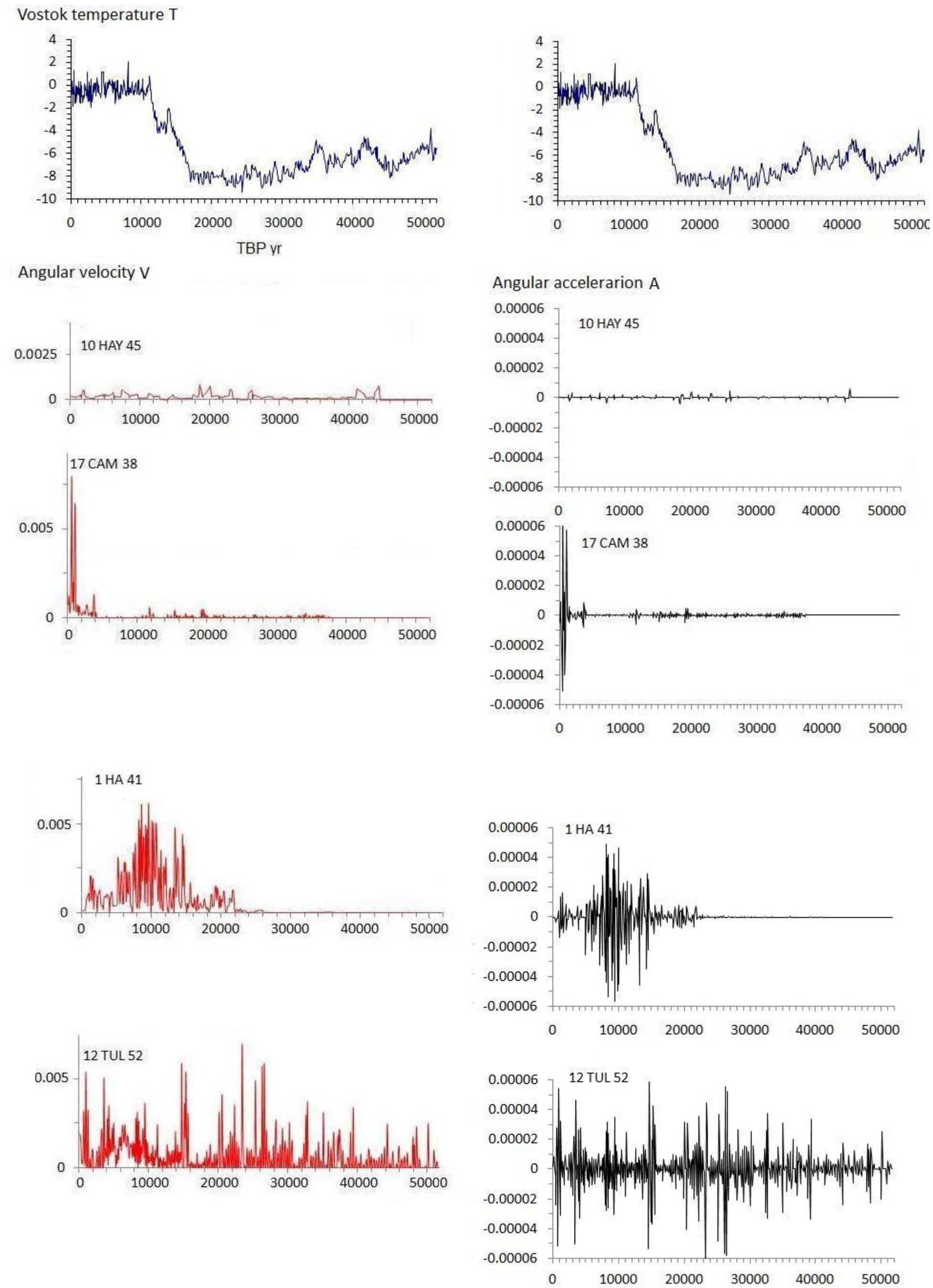

Fig. 3 Basic types of angular velocity *(V)* and acceleration *(A)* oscillations **with the** Vostok temperature graph superimposed. The *V* and *A* graphs are based on equal time steps series. Identification code: case number in Table 1 followed by abbreviated spectrum name and total period length in k yr units. Site and spectrum descriptions are given in Table 1.

We examined the correlative relationship of the oscillations in *V* with temperature oscillations in the Vostok series *T*. We mention the linear relationship of Vostok *T* and the mean global atmospheric surface temperature (Orlóci, 2008) . The correlation analysis is highlighted by three elementary operations: (1) error dampening by sliding windows averaging at window (block) sizes *BS = 1, 2, ..., maxB*, (2) calculation of correlation coefficient *r*(*V*,*T*) at each *BS* on the basis of the averages, and (3) regression analysis to estimate *r*(*V*,*T*) at *BS = 1*.

Figure 4 contains the relevant graphs of regression estimation. The steps are the following: (1) Taking one spectrum at a time, compute an *r*(*V*,*T*) value based on the original *V,T* series for the spectrum. Plot this value at *BS = 1* as in Fig. 4. (2) Increase block size by 1 unit to *B = 2,* then use the block of two units as a sliding window, compute the window average of *V* and *T* in each position and replace the values at the head of the windows by the averages. Move the window through all positions up to *n-1*, obtain the *n-1* valued time series of averages and calculate a new *r*(*V,T*) value. Plot this value at *BS = 2* as in Fig. 4. (3) Continue in like manner incrementing *BS* by 1 unit at a time, in steps, computing new averages for *V* and *T,* and a new *R*(*V,T*) at each step. Plot the results to obtain the full *r*(*V,T*) graph. Our stopping rule for incrementing *BS* is *BS* reaching *n/2* or 40-unit length whichever is the smallest. (4) Fit a linear regression line to the *r*(*V*,*T*) series as in Fig. 4, solve the regression equation y2 for *BS* = 1, and use the solution as best estimate of the correlation coefficient of *V* and *T.* (5) At each *BS* value, sample-and-resample the *V*,*T* series of averages a large number of times, say 1000, involving windows of random length (minimum 5 time steps) laid in random positions. Screen the 1000 *r*(*V,T*) values to determine the relative frequency of positive and negative correlations. Plot these to obtain the F^+ and F^- curves as in Fig. 4. The best estimates of F^+ and F^- are the solutions of regression equations y1 and y3 for *BS = 1.*

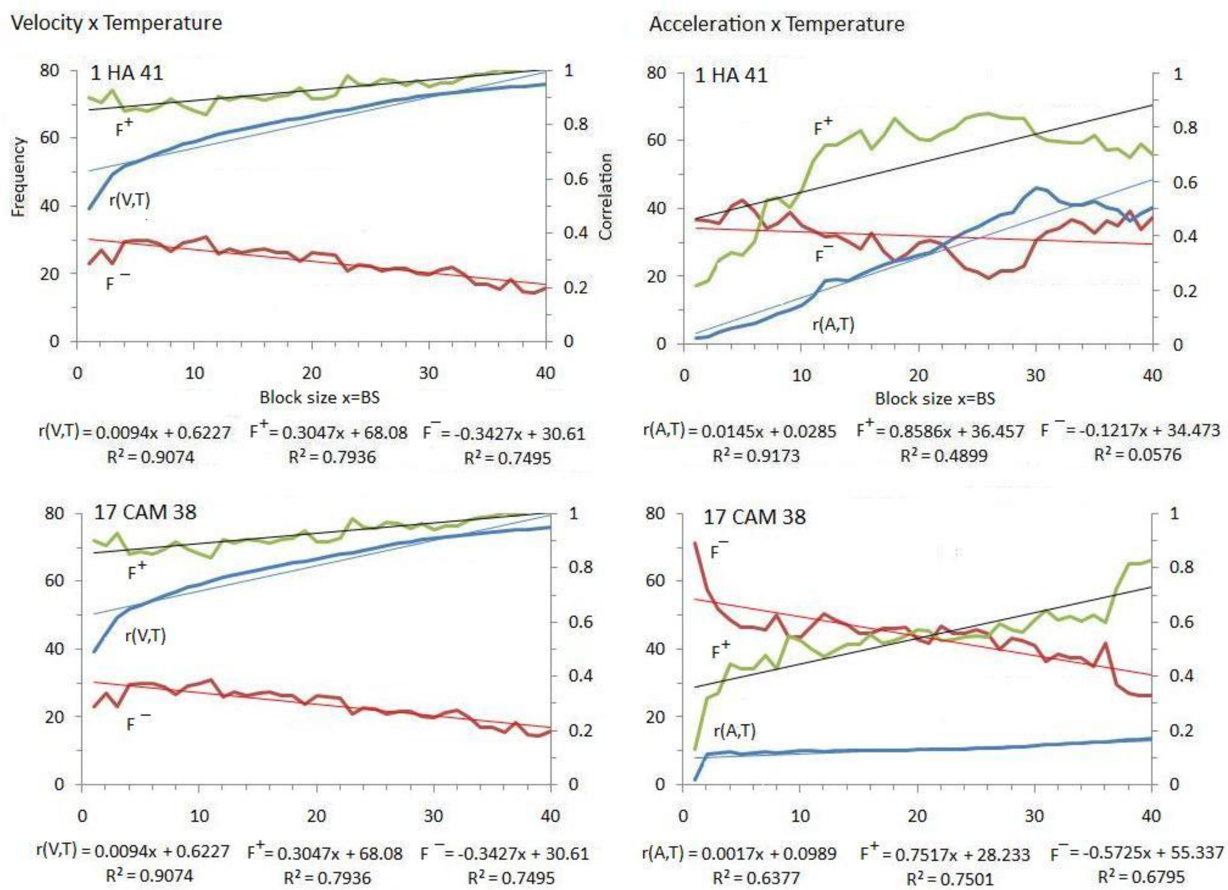

Velocity x Temperature
Acceleration x Temperature
1 HA 41
17 CAM 38
Frequency
Correlation
Block size x=BS
F+
F−
r(V,T)
r(A,T)
r(V,T) = 0.0094x + 0.6227 R² = 0.9074
F+ = 0.3047x + 68.08 R² = 0.7936
F− = -0.3427x + 30.61 R² = 0.7495
r(A,T) = 0.0145x + 0.0285 R² = 0.9173
F+ = 0.8586x + 36.457 R² = 0.4899
F− = -0.1217x + 34.473 R² = 0.0576
r(V,T) = 0.0094x + 0.6227 R² = 0.9074
F+ = 0.3047x + 68.08 R² = 0.7936
F− = -0.3427x + 30.61 R² = 0.7495
r(A,T) = 0.0017x + 0.0989 R² = 0.6377
F+ = 0.7517x + 28.233 R² = 0.7501
F− = -0.5725x + 55.337 R² = 0.6795

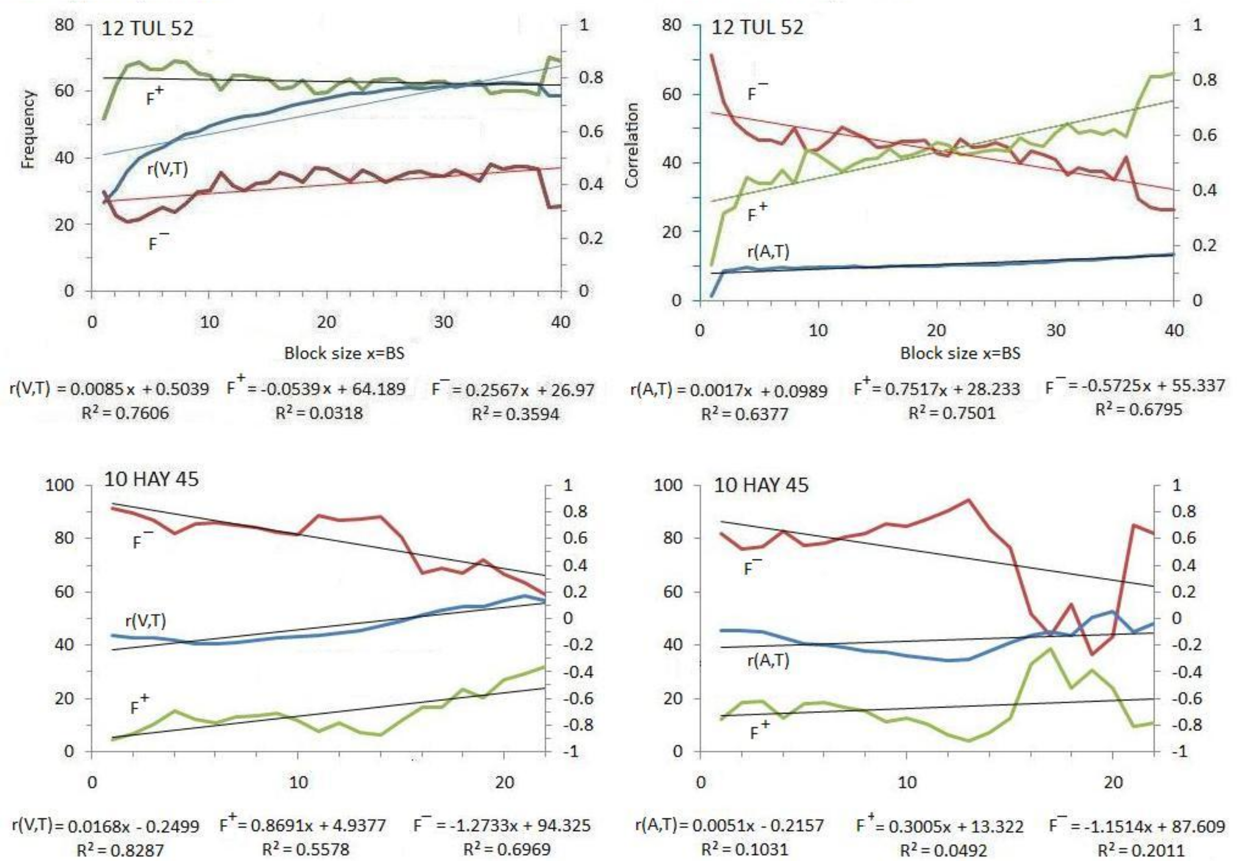

Fig. 4 Estimation of the correlation coefficients *r*(*V*,*T*) and *r*(*A,T* of compositional transition velocity (*V*) and acceleration (*A*) with the Vostok temperature series (*T*), and the correlation coefficients' sign frequencies (F^+, F^-) in the type spectra (Table 3) identified by code in Table 1. The $F^{+,}$ and F^- frequencies are expressed in percentage terms out of 1000 trials. Point estimates are obtained by solving the regression equations for $BS = 1$. R^2 is the coefficient of determination (the amount of the total sum of squares accounted for by regression). See the main text for further details.

4 Results and discussion

We begin this section with process parallelism (Fig. 2). The large volume of relevant numerical results excludes their presentation in the main text, except for the selected cases. The first fact to be mentioned is that the inclusion of scale in the manner of the incremented tolerance radius *TR* enables us to determine the extent to which random variation has to be suppressed in order for the parallelism scalar *TSC* to reach maximum deviation from random expectation *E*. It should be clear too that the *TSC* value can give guidance, but in itself is not adequate. To see this, it is sufficient to consider that there is a basic level of parallelism between any pair of natural or random spectra and this level of parallelism is measured by the *E* quantity. Therefore, it makes sense to use *maxD* as parallelism criterion. This can be expressed in relative terms of the possible maximum (see Fig. 2). Regarding significance, all points of the *TSC* graph outside the probabilistic confidence limits *LL* and *UL* are considered statistically unusually large and for that reason significant. Therefore, the probability discriminating in favour of the global parallelism rule on the top side is $P = 1 - \alpha = 0.975.$ In Fig. 2, the actual *P* values are listed for *maxD.* Considering the entire sample of 23 spectra, we found that all 254 distinct pair wise *maxD* values are highly significant. We consider this as substantive support for the reality of the global parallelism rule.

How do we interpret cases where a portion of the *TSC* graph is below the *E* graph? This question brings up an important finding by P. Greig-Smith concerning the ground pattern of species (Greig-Smith, 1952, 1957). He shows show that pattern in Nature can be more or less intense (aggregated, directed) than the expected *E* in a pure, random walk process. In our case, the Greig-Smith principle translates into stating that there is a base level of parallelism *E* which we expect even in a random process. The actual parallelism *TSC* can be more intense (*TSC* > *E*) or less intensive (*TSC* < *E*) than *E*. Is this some unexplainable paradox? It is not. Chaos theory (Schroeder, 1991) is telling us that order (aggregation, directedness) can arise from randomness on either side of *E.*.The arrangement of the graphs in Fig. 2 reveals several interesting regularities: (1) the *TSC* graph's shape changes from horizontal (line at *TSC = 1,* self comparison) to convex and gradually to strongly concave (random walk). (2) The *maxD* values decrease from 0.66 (self comparison) to close to zero (random walk). The difference from 0 in the random walk case is the bias in the estimation of *maxD*. (3) The *TR* value at which *maxD* occurs keeps increasing from 34% (self comparison) to 67% (random walk). We conclude that the *TSC* metric or equivalently the *maxD* metric is a sensitive indicator of the level of parallelism in compositional transitions.

We used the Sheffé (1953) criterion to compare the mean *maxD* values between ecoregions taken in pairs (Table 2). Sheffé's criterion is $Q_{jm} = \frac{|\Delta_{jm}|}{S_D}$ and further $\Delta_{jm} = \overline{D}_j - \overline{D}_m$ which is the difference of the mean values of *maxD* in ecoregions *j* and *m*. The denominator of *Q* $S_D = \left[S_{EM}^2 \left(\frac{1}{n_j} + \frac{1}{n_m} \right) \right]^{0.5}$ has S_{EM}^2 defined as the global error mean square in the sample of the 254 *maxD* values. Symbols n_j and n_m represent the number of *maxD* values that contributed to the mean in the two ecoregions. We used $F = \frac{Q^2}{k-1}$ for statements of significance, which has the theoretical *F*-distribution with *k-1* and *n-k* degrees of freedom under restrictive conditions specified by Morrison (1976). In Table 2, $k = 6$ and $n = 253$. Mechanistically, we consider a Q_{jm} value significant at the α probability level when the observed *F* value is at least as large as the α probability point of the theoretical *F* distribution.

Considering the matter of significance further, all the *Q* values of Table 2 miss significance by a wide margin, except in the cases *TE*, *TD*, and *S* which contain only one spectrum each. When there is only a single spectrum in an ecoregion, the *maxD* value used is the value from self comparison. But then the test implies an idealised condition of spectral constancy within the ecoregion, not to be expected in nature.

Leaving the comparisons involving *TE*, *TD*, and *S* separate on their own, we conclude that the geographic units we identified as ecoregions do not differ significantly regarding the parallel tendencies of the compositional transitions. This definitely supports the existence of a global co-ordination (paralellism) rule.

Table 2 Comparison of ecoregions (Table 1) based on the *maxD* differences and Sheffé's *Q* statistics

Q values	B	G	D	TS	TE,TD,S*
T	3.142	1.234	1.273	3.193	1.962
B		1.234	1.248	0.232	4.155
G			1.001	1.385	2.186
D				1.173	3.665
TS					4.165
α values (one sided)					
T	0.21	0.97	0.97	0.19	0.77
B		0.97	0.97	1.00	0.024
G			0.19	0.95	0.67
D				0.98	0.98
TS					0.024

*Single *spectrum* per ecoregion. Details regarding *Q* and the associated probabilities α are discussed in the main text. Taking the $\alpha = 0.025$ probability point as a critical limit, each *Q* value in the table misses statistical significance, except the two in the column marked by one asterisk. The latter represent special cases of little practical importance (see text). Symbols: T –Tundra and Taiga; B – Boreal Evergreen; G –Grassland; D – Semi desert (North, South); TS – Tropical Seasonal; TE – Tropical Evergreen; TD– Temperate Seasonal; S – Shrub. All comparisons are based on series with time step width adjusted to 100 yr.

We included the angular velocity and acceleration graphs (*V*, *A*) of the type spectra in Fig. 3. A complete set of the velocity graphs is placed in the Web-based file Appendix L at URL: http://vegetationdynamics.com linking to Appendix GP. The graphs of the periodic means of *V* and corresponding standard deviations are found at the same address in Appendix M. Figure 3 includes the Vostok inversion level temperature graph from Petit et al. (1999). We note that the velocity graphs are based on spectra with time steps adjusted to 100 k yr. The period lengths are not equal, and in some periods zero velocities are registered. The stretches of zero angular velocity probably indicate dates which were stepped over by low-density sampling (see original web based records). The close correlation of velocity fluctuations and global climate warming has been already mentioned (Orlóci, 2009; Orlóci et al., 2002, 2006).

The *V* graphs of the different spectra considerably, but still not so individualistically that we could not recognize major morphological types (Fig. 3, Table 3). The first dichotomy separates spectra whose velocity graphs have very low amplitudes (a1) compared to the other graphs which at least during some time period show high amplitude velocity changes (a2). The a2 group includes three subgroups of spectra: a21 — low amplitude velocity oscillations during the Ice Age and explosively high velocity oscillations after rapid climate warming; a22 — explosive high velocity oscillations dispersed through the entire glacial and interglacial period; a23 — high velocity peaks during the recent 500 or 600 years. Web-based Appendix M (see URL above) has the banner graphs which further clarify the manner of angular velocity oscillations in terms of periodic averages and standard deviations.

Table 3 Classification of spectra according to the shape of the velocity graph *

type	type spectra	comments
a11	10 HAY 45	Low velocity is general, negative *V*, *T* correlation dominant.
a12	15 LDP 45	Low velocity is general, positive *V*, *T* correlation dominant.
a21	1 HA 45	Velocity low-level earlier, explosive assent later.
a22	12 TUL 52	Explosive velocity oscillations dispersed over entire period.
a23	17 COM 38	Explosive velocity rise in recent centuries.

*****Figure 3 illustrates typical graphs. A complete set of graphs is placed into the Web-based Appendix GP (see URL in the text). See Table 1 and Fig. 3 for code to spectra.

We discussed the broader environmental significance of the *V*,*T* correlations at length in earlier papers (Orlóci et al., 2006; Orlóci, 2009). The results presented in the top portion of Table 4 confirm the earlier conclusions. As could be expected, the Tundra (Hanging Lake) and the subtropical Lake Tulan spectra dominate the F^+ column in the V,T portion of Table 4. The Hay Lake spectrum is sharply separated from the other spectra by dominating the F^- column in both the V,T and A,T portions. The ordering of the type spectra by the F^+ column in the A,T portion only faintly resembles the ordering in the V,T portion of Table 4. This suggests the blurring of the climatic connection by the acceleration scalar and a boost to randomness. But then as a second derivative, the acceleration scalar does a superb job to pinpoint the hotspots of change.

Table 4 Regression constants and estimates of correlation $r(V,T)$, $r(A,T)$ and their sign frequencies (F^+ and F^-) in the type spectra of Figure 3.*

Compositional transition velocity

spectrum	c	b	$r(V,T)$	c	b	F^-	c	b	F^+
1 HA 45	0.632	0.009	0.641	30.268	–0.343	29.925	68.400	0.305	**68.705**
12 TUL 52	0.504	0.009	0.513	26.970	0.257	27.227	64.189	–0.054	**64.135**
17 CAM 38	0.524	0.005	0.529	33.242	–0.470	32.772	55.907	0.721	**56.628**
10 HAY 45	–0.250	0.017	–0.233	95.302	–1.396	**93.906**	3.723	1.021	**4.744**
Mean	0.353	0.010	0.363	46.4455	–0.488	45.9575	48.05475	0.49825	**48.553**

Compositional transition acceleration

spectrum	c	b	$r(A,T)$	c	b	F-	c	b	F^+
1 HA 45	0.029	0.015	0.044	34.474	–0.122	34.352	36.458	0.859	37.317
17 CAM 38	–0.008	0.003	–0.005	36.899	–0.666	36.233	24.742	1.433	26.175
12 TUL 52	0.100	0.002	0.102	55.338	–0.573	54.765	28.234	0.752	28.986
10 HAY 45	–0.215	0.005	–0.210	87.609	–1.151	86.458	13.322	0.300	13.622
Mean	–0.024	0.006	–0.017	53.580	–0.628	52.952	25.689	0.836	26.525

*The regression graphs are in Fig. 4. The method follows Orlóci et al. (2006). The estimates are given for block size 1 and are based on the original records without equal time step transformations. Symbols *b* and *c* represent the regression coefficient and the *y* axis intercept.

5 Closing remarks

We stated with two propositions about process governance in the long-term vegetation process. The first proposition suggests that the parallelism of compositional transitions is a global rule. In support of this rule, we pointed to the generally low *P* values, and equivalently, to the highly significant *maxD* values. We concluded from these that the global parallelism rule transcends ecoregional variability.

The second proposition brought up the question of the locality of compositional instability. We found regularities in the transition velocity statistics and in the clearly defined variability of correlations of compositional transition velocity and the Vostok atmospheric temperature series which are trans-ecoregional. This supports the existence of a strong local rule which governs compositional instability.

What can we infer from having parallelism as a global rule and compositional instability as a local rule in the current climate warming cycle (IPCC reports, 2001, 2007)? They tell us that there is no region whose vegetation could escape the consequences of climate warming, but we have to expect sensitive differences in the intensity of vegetation response depending on the loca conditions. For example, the destabilization effect that brings catastrophic change into high latitude regions (Orlóci, 1994, 2008 and references therein) may not bring the same results into others.

Multiscaling and experimental empiricism are our two pillars of statistical testing. Multiscaling helps to pinpoint the time step width at which process parallelism most clearly appears or the *VT* and *AT* correlations are strongest. Put it in another way, by manipulation of the scale we can find the limit to which random variation has to be suppressed by averaging or changes in the tolerance radius to optimize the appearance of important process regularities. Optimization by averaging has precedents in statistical ecology. We point, for examples, to Greig-Smith's (1952) pattern analysis and to the edge detection technique of different authors (Orlóci and Orlóci, 1990; and references therein).

References

Anderson P M (1985). Late Quaternary vegetational change in the Kotzebue Sound area, northwestern Alaska. Quaternary Research, 24: 307--321

Anderson P M (1988). Late Quaternary pollen records from the Kobuk and Noatak River drainages, northwestern Alaska. Quaternary Research, 29: 263--276

Behling H (1995). Investigations into the Late Pleistocene and Holocene history of vegetation and climate in Santa Catarina (S Brazil). Vegetation History and Archaeobotany, 4: 127--152

Behling H (1997a). Late Quaternary vegetation, climate and fire history from the tropical mountain region of Morro de Itapeva, SE Brazil. Palaeogeography, Palaeoclimatology Palaeoecology, 129: 407--422

Behling H (1997b). Late Quaternary vegetation, climate and fire history in the Araucaria forest and campos region from Serra Campos Gerais (Paraná), S Brazil. Review of Palaeobotony and Palynology, 97: 109--121

Behling H V, Pillar D, Orlóci L, Bauermann S G (2004). Late Quaternary Araucaria forest, grassland (Campos), fire and climate dynamics, studied by high-resolution pollen, charcoal and multivariate analysis of the Cambará do Sul core in southern Brazil. Paleogeography, Paleoclimatology, Paleoecology, 203: 277--297

Bryant V M, Jr (1977). A 16,000 year pollen record of vegetational change in central Texas. Palynology, 1: 143--156

Colinvaux P A , de Oliveira P E, Moreno J E, Miller M C, Bush M B (1996). A long pollen record from lowland Amazonia: forest and cooling in glacial times. Science 274: 85-88.

Cwynar L C (1982). A Late-Quaternary vegetation history from Hanging Lake, northern Yukon. Ecological Monographs, 52: 1-24.

Fredlund G G (1995). Late Quaternary pollen record from Cheyenne Bottoms, Kansas. Quaternary Research, 43: 67--79

Greig-Smith P (1952). The use of random and contiguous quadrats in the study of the structure of plant communities. Annals of Botany, 16: 293--316

Greig-Smith P (1957). Quantitative Plant Ecology. Butterworth, Oxford. 983 ed. Oxford: Blackwell Scientific

Grimm E C, Jacobson, G L Jr, Watts W A, Hansen B C S, Maasch K A (1993). A 50,000-year record of climate oscillations from Florida and its temporal correlation with the Heinrich events. Science, 261: 198-200.

Hammersley J M, Handscomb D C (1964). Monte Carlo Methods. London: Methuen.

He X S, Orlóci L (1999). Anderson Pond revisited: the late Quaternary vegetation process. Abstracta Botanica. Abstracta Botanica, 22: 81--93

Intergovernmental Panel on Climate Change (IPCC) (2001). Third Assessment Report – Climate Change. URL: http://www.ipcc.ch

Intergovernmental Panel on Climate Change (IPCC) (2007). Fourth Assessment Report – Climate hange. URL: http://www.ipcc.ch

Jacobs B F (1985). A middle Wisconsin pollen record from Hay Lake, Arizona. Quaternary Research 24: 121-130.

Lapola D M, Oyama M D, Nobre C A, Sampaio G (2008). A new world natural vegetation map for global change studies. Anais da Academia Brasileira de Ciencias vol. 80 no. 2, Rio de Janeiro, Brasil. URL: www.scielo.br/scielo.php?script=sci_arttext&pid=S0001-37652008000200017

Markgraf V (1983). Late and Postglacial vegetational and paleoclimatic changes in subantarctic, temperate, and arid environments in Argentina. Palynology, 7: 43--70

Markgraf V (1987). Paleoenvironmental changes at the northern limit of the subantarctic Nothofagus forest, latitude 37°S, Argentina. Quaternary Research, 28: 119--129

Markgraf V (1989). Late Pleistocene/Holocene paleoclimates from subantarctic latitudes. Antarctic Journal of the United States, 24(5): 1--2

Matthews J V Jr (1980). Paleoecology of John Klondike Bog, Fisherman Lake region, southwest district of Mackenzie. Geological Survey of Canada Paper, 80--22

McAndrews J H (1981). Late Quaternary climate of Ontario: temperature trends from the fossil pollen record. In: Mahaney W C, ed. Quaternary Paleoclimate. Norwich, England: Geo Abstracts, Ltd., 319--333

Morrison D F (1976). Multivariate Statistical Methods. London: McGraw-Hill, 415

Orlóci L (1991). On character-based plant community analysis: choice, arrangement, comparison. Coenoses, 6: 103--107

Orlóci L (1994). Global warming: the process and its anticipated phytoclimatic effects in temperate and cold zones. Coenoses, 9: 69--74

Orlóci L (2008). Vegetation displacement issues and transition statistics in climate warming cycle. Community Ecology, 9: 83--98

Orlóci L (2009). Multi-scale trajectory analysis: powerful conceptual tool for understanding ecological change. Volume 4, No. 2, March. OnlineFirst at: http://www.springerlink.com/content/p2777845u7174262/?p=12d64f7280af47a1b44b0799bb0fc137&pi=0

Orlóci L, Orlóci M (1990). Edge detection in vegetation: Jornada revisited. Journal of Vegetation Science, 1: 311--324

Orlóci L, Pillar V D, Anand M (2006). Multiscale analysis of palynological records: new possibilities. Community Ecology, 7: 53--68

Orlóci L, Pillar V D, Anand M, Behling H (2002). Some interesting characteristics of the vegetation process. Community Ecology, 3: 125--146

Petit J R, Jouzel D, Raynaud D, Barkov N I, Barnola J M, Basile I, Bender M, Chappellaz J, Davis J, Delaygue G, Delmotte M, Kotlyakov V M, Legrand M, Lipenkov V, Lorius C, Pepin L, Ritz C, Saltzmann E, Stievenard M (1999). Climate and atmospheric history of the past 420,000 years from the Vostok Ice Core, Antarctica. Nature, 300: 429--436

Pillar V D, Orlóci L (1993a). Character-based Vegetation Analysis: the Theory and an Application Program. Ecological Computations Series (ECS): Vol. 5. SPB Academic Publishing bv, The Hague, The Netherlands.

Pillar V D, Orlóci L (1993b). Taxonomy and perception in vegetation analysis. Coenoses 8: 53-66.

Von Post L (1946). The prospect for pollen analysis in the study of the earth climatic history. New Phytol, 45: 193--217

Ritchie J C (1976). The late-Quaternary vegetational history of the western interior of Canada. Canadian Journal of Botany, 54: 1793-1818.

Ritchie J C (1964). Contributions to the Holocene paleoecology of westcentral Canada. I. The Riding Mountain area. Canadian Journal of Botany, 42: 181--197

Salgado-Labouriau M L (1988). Sequence of colonization by plants in the Venezuelan Andes after the last Pleistocene glaciation. Journal of Palynology, 23/24: 189--204

Schroeder M (1991). Fractals, chaos, Power Laws. Minutes from an Infinite Paradise. Freeman, New York..

Watts W A, Bradbury J P (1982). Paleoecological studies at Lake Patzcuaro on the west-central Mexican Plateau and at Chalco in the Basin of Mexico. Quaternary Research 17: 56-70.